Pch2 Modulates Chromatid Partner Choice During Meiotic Double-Strand Break Repair in *Saccharomyces cerevisiae*

Sarah Zanders,[1] Megan Sonntag Brown, Cheng Chen, and Eric Alani[2]
Department of Molecular Biology and Genetics, Cornell University, Ithaca, New York 14853-2073

ABSTRACT In most organisms, the segregation of chromosomes during the first meiotic division is dependent upon at least one crossover (CO) between each pair of homologous chromosomes. COs can result from chromosome double-strand breaks (DSBs) that are induced and preferentially repaired using the homologous chromosome as a template. The *PCH2* gene of budding yeast is required to establish proper meiotic chromosome axis structure and to regulate meiotic interhomolog DSB repair outcomes. These roles appear conserved in the mouse ortholog of *PCH2*, *Trip13*, which is also involved in meiotic chromosome axis organization and the regulation of DSB repair. Using a combination of genetic and physical assays to monitor meiotic DSB repair, we present data consistent with *pch2*Δ mutants showing defects in suppressing intersister DSB repair. These defects appear most pronounced in *dmc1*Δ mutants, which are defective for interhomolog repair, and explain the previously reported observation that *pch2*Δ *dmc1*Δ cells can complete meiosis. Results from genetic epistasis analyses involving *spo13*Δ, *rad54*Δ, and *mek1*/*MEK1* alleles and an intersister recombination reporter assay are also consistent with Pch2 acting to limit intersister repair. We propose a model in which Pch2 is required to promote full Mek1 activity and thereby promotes interhomolog repair.

DNA double-strand breaks (DSBs) that occur during vegetative growth are preferentially repaired via homologous recombination in which the Rad51 recombinase and its partner Rad54 mediate strand exchange with the sister chromatid. This intersister repair occurs even in diploid cells where a homologous chromosome template is available and is thought to help prevent chromosome rearrangements (Kadyk and Hartwell 1992; M. Shinohara *et al.* 1997; Arbel *et al.* 1999; Krogh and Symington 2004). In meiosis, formation of programmed DSBs and their repair using the homologous chromosome as a template is essential for the production of viable gametes (Roeder 1997). Although Rad51 and Rad54 are still present, meiotic interhomolog strand exchange is accomplished by their respective orthologs, Dmc1 and Rdh54 (Dresser *et al.* 1997; Klein 1997; A. Shinohara *et al.* 1997; M. Shinohara 1997; Arbel *et al.* 1999; Hollingsworth 2010). Interhomolog DSB repair creates linkages provided by genetic exchanges, or crossovers (COs), between homologous chromosomes. In many organisms, these COs are required for reductional chromosome segregation at the meiosis I (MI) division, which lowers cell ploidy by one-half, allowing for the generation of haploid gametes (Roeder 1997). If any pair of homologous chromosomes fails to receive a CO, MI nondisjunction can occur and produce aneuploid gametes, which cause conditions such as Down syndrome or infertility in humans (Hassold *et al.* 2007).

During meiotic prophase I in budding yeast, ~140–170 DNA DSBs are introduced into the genome by a group of 10 proteins, of which Spo11 is the catalytic component (Blitzblau *et al.* 2007; Buhler *et al.* 2007; Mancera *et al.* 2008). Although COs are the only repair products known to promote MI disjunction, only ~50% of DSBs in yeast meiosis are repaired as interhomolog COs. Some DSBs are repaired using the homologous chromosome without producing a CO; this is known as a noncrossover (NCO). Obligate CO formation, CO interference, and CO homeostasis are manifestations of interhomolog DSB repair regulation acting to ensure each pair of homologous chromosomes disjoins at

doi: 10.1534/genetics.111.129031
Manuscript received December 13, 2010; accepted for publication April 11, 2011
[1]Present address: Division of Basic Sciences, Fred Hutchinson Cancer Research Center, Mail Stop A2-025, P.O. Box 19024, Seattle, WA 98109-1024.
[2]Corresponding author: Department of Molecular Biology and Genetics, 459 Biotechnology Bldg., Cornell University, Ithaca, NY 14853-2703. E-mail: eea3@cornell.edu

MI (Bishop and Zickler 2004; Borner *et al.* 2004; Martini *et al.* 2006; Blitzblau *et al.* 2007; Buhler *et al.* 2007; Chen *et al.* 2008; Mancera *et al.* 2008; Berchowitz and Copenhaver 2010). The obligate CO refers to the observation that all homologous chromosome pairs receive at least one CO. CO interference describes the nonrandom, evenly spaced distribution of CO events, and CO homeostasis describes the finding that CO levels are maintained as DSB frequencies decrease (reviewed in Jones and Franklin 2006; Berchowitz and Copenhaver 2010). Little is known about the mechanisms or relatedness of the different aspects of CO control, although one mutant, *pch2*Δ, has decreased CO interference and may also be defective for CO homeostasis (Joshi *et al.* 2009; Zanders and Alani 2009).

The ~10–33% of meiotic DSBs estimated to not be repaired using a homologous chromosome are repaired by homologous recombination using the sister chromatid as a template (*e.g.*, Goldfarb and Lichten 2010). The shift in DSB repair template preference from the sister chromatid in the mitotic cell cycle to the homologous chromosome in meiosis is referred to as "interhomolog bias" (Jackson and Fink 1985; Schwacha and Kleckner 1994, 1997; Wan *et al.* 2004; Webber *et al.* 2004; Niu *et al.* 2005, 2007, 2009; Goldfarb and Lichten 2010). Interhomolog bias is established shortly after DSB formation and requires components of the axial elements, which are linear structures that form along each pair of sister chromatids early in meiotic prophase (Hollingsworth 2010). An early step in instituting interhomolog bias is phosphorylation of Hop1 of the Hop1/Red1 axial element duo by the Mec1 and Tel1 kinases (Hollingsworth and Byers 1989; Hollingsworth *et al.* 1990; Rockmill and Roeder 1990; Carballo *et al.* 2008). Red1 and phosphorylated Hop1 are required for the activation of the effector kinase Mek1 (Niu *et al.* 2005, 2007; Carballo *et al.* 2008). Mek1 appears to directly promote interhomolog repair (Terentyev *et al.* 2010). In addition, Mek1 phosphorylates Rad54, which inhibits the interaction between Rad51 and Rad54 (Niu *et al.* 2009). Phosphorylation of Rad54 contributes to, but is not sufficient for, complete interhomolog bias (Niu *et al.* 2009). The meiosis-specific protein Hed1 also acts to prevent Rad51–Rad54 complex formation by competing with Rad54 for Rad51 binding, although the role of Hed1 in interhomolog bias is yet to be determined (Tsubouchi and Roeder 2006; Busygina *et al.* 2008). Interhomolog bias is maintained in haploid meiosis and inhibits DSB repair, suggesting that interhomolog interactions are not required (Demassy *et al.* 1994; Callender and Hollingsworth 2010). At hemizygous DSB sites in diploid meiosis, intersister repair is constrained by a Mek1-dependent delay, although efficient intersister DSB repair does occur (Goldfarb and Lichten 2010).

The mechanisms promoting interhomolog bias are often studied in *dmc1* null mutant backgrounds in which unrepaired DSBs trigger the meiotic recombination checkpoint to arrest cells at pachytene, the last stage of meiotic prophase before cells are committed to undergo the MI division (Hollingsworth 2010). There are two ways in which recombination checkpoint arrest can be overcome in a *dmc1* mutant background. The first is to eliminate any of the essential recombination checkpoint genes such as *MEC1, RAD17*, or *RAD24*. In such cases, meiosis proceeds with unrepaired breaks to form inviable gametes (Lydall *et al.* 1996). The second is to eliminate (or reduce; see below) the checkpoint-eliciting DNA lesions either by preventing DSB formation or by allowing inappropriate Dmc1-independent DSB repair (Bishop *et al.* 1992, 1999; Schwacha and Kleckner 1994, 1997; Xu *et al.* 1997; Thompson and Stahl 1999). The latter can be accomplished by several mechanisms. Overexpressing *RAD51* or *RAD54* and/or mutating *HED1* in a *dmc1* background allows for meiotic progression and the production of moderate to wild-type levels of interhomolog COs and thus of viable spores (Bishop *et al.* 1999; Tsubouchi and Roeder 2003, 2006; Busygina *et al.* 2008). Alternatively, when *RED1, HOP1*, or *MEK1* are mutated, interhomolog bias is lost and DSBs are rapidly repaired via Rad51–Rad54-dependent strand exchange using the sister chromatid as a template, and meiosis progresses to produce inviable spores (Bishop *et al.* 1999; Wan *et al.* 2004; Niu *et al.* 2005, 2007).

Pch2 (*p*achytene *ch*eckpoint) is a putative AAA ATPase that promotes the checkpoint arrest/delays observed in *zip1, rad17, mms4*, and *sae2* recombination mutants. The *pch2*Δ mutation also suppressed the *dmc1*Δ checkpoint arrest in some but not all studies (San-Segundo and Roeder 1999; Zierhut *et al.* 2004; Hochwagen *et al.* 2005; Wu and Burgess 2006; Mitra and Roeder 2007; Zanders and Alani 2009). In budding yeast, Pch2 is also required for wild-type kinetics of meiotic progression, CO interference, and establishing proper organization of Hop1 and Zip1 on meiotic chromosomes (Sym and Roeder 1995; Borner *et al.* 2008; Joshi *et al.* 2009; Zanders and Alani 2009). Several of these roles appear conserved in the mouse *PCH2* ortholog *Trip13*, which is required for wild-type levels of DSB repair, wild-type CO distribution, and proper organization of HORMADs (which share homology with Hop1) and the synaptonemal complex central element protein SYCP1 on meiotic axes (Li and Schimenti 2007; Wojtasz *et al.* 2009; Roig *et al.* 2010).

Here we investigated the mechanisms by which the *pch2*Δ mutation suppresses the meiotic arrest/delay phenotypes of *dmc1*Δ mutations. First, we found that lowering DSB levels in *dmc1*Δ mutants reduced the fraction of cells that arrest, indicating that the recombination checkpoint is sensitive to DSB levels. Second, we found that Pch2 inhibited some DSB repair in *dmc1*Δ cells that likely includes, but may not be limited to, intersister recombination. Third, we identified genetic interactions between *PCH2* and *RAD54* and *PCH2* and *MEK1* that support a role for Pch2 in limiting intersister repair. Finally, we present a genetic assay that demonstrates an increase in intersister repair at one locus in *pch2*Δ mutants. We synthesize our data with published results to propose a model in which Pch2 is required for full Mek1 activity.

Materials and Methods

Media and yeast strains

All yeast strains (Table 1) were grown at 30° on yeast peptone dextrose (YPD) supplemented with complete amino acid mix, synthetic complete, or synthetic complete −histidine (Argueso *et al.* 2004). All strains were sporulated at 30°. The sporulation media and sporulation conditions used to generate the data in Tables 2–4 were described previously (Zanders and Alani 2009). Differences in spore formation and viability were analyzed by a χ^2 test in which *P*-values <0.05 were considered statistically significant. Geneticin (Invitrogen), nourseothricin (Hans-Knoll Institute fur Naturstoff-Forschung), and hygromycin B (Calbiochem) were added in standard concentrations to YPD media when required (Wach *et al.* 1994; Goldstein and McCusker 1999).

Strains described in Tables 2 and 3 are isogenic to the NHY943 or NHY942 SK1 strains described in de los Santos *et al.* (2003). The *spo11* hypomorphic mutants and the NHY943 strains containing these alleles are described in Martini *et al.* (2006). As in Martini *et al.* (2006), we refer to *spo11-HA3His6* as *spo11-HA*. The *dmc1*Δ and *rad54*Δ alleles used in this work were all complete open reading frame deletions. The *pch2*Δ allele contains a deletion of amino acids 17–587 (Zanders and Alani 2009). All deletion cassettes were made via PCR, and the deleted regions were replaced with *HPHMX4, KANMX4*, or *NATMX4* as shown in Table 1. A *Bam*HI fragment of pNKY58 was integrated into the genome to create the *spo13::hisG-URA3-hisG* mutation, and a *Bgl*II to *Eco*RI fragment of pNKY349 was used to replace *RAD50* with *rad50S::URA3* (Alani *et al.* 1990). All mutations were initially integrated into the genome using standard transformation techniques (Gietz *et al.* 1995). Standard genetic crosses were used to generate the various mutant combinations. Details on strain construction and primer sequences are available upon request.

The *pch2*Δ *spo11-HA mek1-as* and *pch2*Δ *spo11-HA MEK1-GST* strains presented in Table 4 were constructed as follows. The *mek1-as* strain was constructed by digesting the plasmid pJR2 with *Rsr*II and then by transforming the *mek1-Q241G::URA3* segment into the *ura3 mek1*Δ SK1 diploid YTS1 (plasmid and strain provided by Nancy Hollingworth). The diploid was then tetrad-dissected, selecting for Ura$^+$ haploid segregants. The homozygous *MEK1-GST* diploid SK1 strain SBY2901 (provided by Sean Burgess) was also tetrad-dissected to obtain haploid segregants. The *mek1-as* and *MEK1-GST* segregants described above were mated to EAY2581 (*pch2*Δ), EAY2263 (*pch2*Δ *spo11-HA*), and SKY635 (*spo11-HA*). The resulting diploids were sporulated and tetrad-dissected to obtain the haploids in Table 1 that were then mated to create diploids that were tetrad-dissected.

To create the strains used in the sister-chromatid exchange assays, the *HIS3* gene was deleted from a haploid segregant of the SK1 diploid EAY28 to create EAY2908. A cross of EAY2908 by EAY2209 (*pch2*Δ in NHY943) (Zanders and Alani 2009) generated EAY2910 and EAY2913. The *HIS3* sister-chromatid recombination reporter assay contained on plasmid pNN287 (provided by Mike Fasullo) was integrated into the genome near *TRP1* in EAY2913, as described by Fasullo and Davis (1987), to create EAY2918. Correct integration of the sister-chromatid recombination assay in EAY2918 was confirmed using Southern blot analysis. EAY2918 was then crossed to EAY2910 to generate strains EAY2951 and EAY2952 (wild type) and EAY2955 and EAY2956 (*pch2*Δ) used in the sister-chromatid recombination experiments.

To measure sister-chromatid recombination, saturated YPD overnight cultures were diluted into 22 ml YPA and grown for 17 hr. A sample of each YPA culture (0.4–2 ml) was plated on synthetic complete −HIS plates to detect early mitotic sister-chromatid recombination events that would skew meiotic analyses. No such His$^+$ jackpots were observed in cells plated from YPA cultures (generally, fewer than one His$^+$ cell/ml plated was observed for all strains). After 17 hr, the YPA cultures were spun down, washed once in 1% potassium acetate, resuspended in 10 ml 1% potassium acetate, and then allowed to sporulate 24 hr. Undiluted sporulated cells were then plated on synthetic complete −HIS, and cell dilutions were plated on synthetic complete media. The frequency of His$^+$ colony-forming units (cfu) (His$^+$ prototrophy in sporulated cells in which spores in asci were not separated) was found by dividing the number of His$^+$ cfu/ml by the total number of colony-forming units per millimeter. Experimental replicates in which <90% of cells sporulated were not included in the data presented.

Meiotic time courses and DSB Southern blotting

For the time courses to analyze meiotic DSB levels, 0.3 ml (for *RAD54* strains) or 0.6 ml (for *rad54*Δ strains) of a saturated YPD overnight culture from each strain to be analyzed was diluted into 200 ml YPA (2% potassium acetate) plus complete amino acid mix and grown for 17 hr. The YPA culture was then spun down, washed once in 1% potassium acetate, and resuspended in 100 ml 1% potassium acetate (Zanders and Alani 2009). All strains were grown in the same batches of media and treated identically. DNA was isolated from meiotic cultures as in Buhler *et al.* (2007) for *dmc1*Δ strains and as in Goyon and Lichten (1993) for *rad50S* strains. The percentage of DSBs was calculated using Image Quant software. In this analysis, a lane profile was generated and used to calculate the total lane signal. Lane background was determined from the blot regions below DSB signals. Only the peaks above lane background were quantified as DSB-specific signals.

Results

*pch2*Δ *suppresses dmc1*Δ *arrest by allowing DSB repair*

We initiated this study in SK1 budding yeast to examine a role for Pch2 in ensuring a meiotic arrest/delay in the absence of Dmc1 (San-Segundo and Roeder 1999; Zierhut *et al.* 2004;

Table 1 Yeast strains used in this study

Strain	Genotype
NH943/EAY2580	*MAT***a**/α, homozygous for: *ho::hisG ade2Δ, ura3(ΔSma-Pst), leu2::hisG, CEN3::ADE2, lys5-P, cyh2^r, his4-B*
EAY2581/EAY2210	as NH943/EAY2580 except *pch2Δ::NATMX4*
EAY2582/SKY635	as NH943/EAY2580 except *spo11-HA3His6::KANMX4*
EAY2787/EAY2263	as NH943/EAY2580 except *pch2Δ::NATMX4, spo11-HA3His6::KANMX4*
EAY2637/EAY2638	as NH943/EAY2580 except *dmc1Δ::KANMX4*
EAY2639/EAY2640	as NH943/EAY2580 except *pch2Δ::NATMX4, dmc1Δ::KANMX4*
EAY2619/EAY2630	as NH943/EAY2580 except *spo11-HA3His6::KANMX4, dmc1Δ::KANMX4*
EAY2631/EAY2632	as NH943/EAY2580 except *pch2Δ::NATMX4, spo11-HA3His6::KANMX4, dmc1Δ::KANMX4*
EAY2582/SKY665	as NH943/EAY2580 except *spo11-HA3His6::KANMX4/spo11(Y135F)-HA3His6::KANMX4*
EAY2787/EAY2265	as NH943/EAY2580 except *pch2Δ::NATMX4, spo11-HA3His6::KANMX4/spo11(Y135F)-HA3His6::KANMX4*
EAY2620/EAY2800	as NH943/EAY2580 except *spo11-HA3His6::KANMX4/spo11(Y135F)-HA3His6::KANMX4, dmc1Δ::KANMX4*
EAY2622/EAY2802	as NH943/EAY2580 except *pch2Δ::NATMX4, spo11-HA3His6::KANMX4/spo11(Y135F)-HA3His6::KANMX5, dmc1Δ::KANMX4*
EAY2589/EAY2590	as NH943/EAY2580 except *spo13::URA3*
EAY2591/EAY2592	as NH943/EAY2580 except *pch2Δ::NATMX4, spo13::URA3*
EAY2595/EAY2596	as NH943/EAY2580 except *spo11-HA3His6::KANMX4, spo13::URA3*
EAY2593/EAY2594	as NH943/EAY2580 except *pch2Δ::NATMX4, spo11-HA3His6::KANMX4, spo13::URA3*
EAY2643/EAY2644	as NH943/EAY2580 except *dmc1Δ::KANMX4, spo13::URA3*
EAY2641/EAY2642	as NH943/EAY2580 except *pch2Δ::NATMX4, dmc1Δ::KANMX4, spo13::URA3*
EAY2633/EAY2634	as NH943/EAY2580 except *spo11-HA3His6::KANMX4, dmc1Δ::KANMX4, spo13::URA3*
EAY2635/EAY2636	as NH943/EAY2580 except *pch2Δ::NATMX4, spo11-HA3His6::KANMX4, dmc1Δ::KANMX4, spo13::URA3*
EAY2578/EAY2579	as NH943/EAY2580 except *rad50S::URA3*
EAY2585/EAY2586	as NH943/EAY2580 except *pch2Δ::NATMX4, rad50S::URA3*
EAY2587/EAY2588	as NH943/EAY2580 except *spo11-HA3His6::KANMX4, rad50S::URA3*
EAY2583/EAY2584	as NH943/EAY2580 except *pch2Δ::NATMX4, spo11-HA3His6::KANMX4, rad50S::URA3*
EAY2722/EAY2723	as NH943/EAY2580 except *rad54Δ::HPHMX4*
EAY2681/EAY2746	as NH943/EAY2580 except *pch2Δ::NATMX4, rad54Δ::HPHMX4*
EAY2740/EAY2741	as NH943/EAY2580 except *spo11-HA3His6::KANMX4, rad54Δ::HPHMX4*
EAY2726/EAY2727	as NH943/EAY2580 except *pch2Δ::NATMX4, spo11-HA3His6::KANMX4, rad54Δ::HPHMX4*
EAY2742/EAY2743	as NH943/EAY2580 except *rad54Δ::HPHMX4, dmc1Δ::KANMX4*
EAY2728/EAY2729	as NH943/EAY2580 except *pch2Δ::NATMX4, rad54Δ::HPHMX4, dmc1Δ::KANMX4*
EAY2738/EAY2739	as NH943/EAY2580 except *spo11-HA3His6::KANMX4, rad54Δ::HPHMX4, dmc1Δ::KANMX4*
EAY2724/EAY2725	as NH943/EAY2580 except *pch2Δ::NATMX4, spo11-HA3His6::KANMX4, rad54Δ::HPHMX4, dmc1Δ::KANMX4*
NH942	*MATα, ho::hisG, ade2Δ, can1, ura3(ΔSma-Pst), met13-B, trp5-S, CEN8::URA3, thr1-A, cup1^S*
EAY2209/EAY2210	as NH942/NH943 except *pch2Δ::NATMX4*
EAY2681/EAY2685	as NH942/NH943 except *pch2Δ::NATMX4, rad54Δ::HPHMX4*
EAY2951/EAY2952	*MAT***a**/α homozygous for *ho::hisG, ura3*, and *his3Δ::KANMX4* hemizygous for *his3-Δ5′ his3-Δ3′::URA3*
EAY2955/EAY2956	as EAY2951/2952 except *pch2Δ::NATMX4*
EAY3077	*MAT***a**, *ho::hisG, leu2*
EAY3078	*MATα, ho::hisG, leu2*
EAY3079	*MAT***a**, *ho::hisG, HIS4, lys5-P, mek1Δ::LEU2::mek1Q241G::URA3*
EAY3080	*MATα, ho::hisG, HIS4, mek1Δ::LEU2::mek1Q241G::URA3*
EAY3081	*MATa, ho::hisG, HIS4, lys5-P, mek1Δ::LEU2::mek1Q241G::URA3, pch2Δ::NATMX4*
EAY3082	*MATα, ho::hisG, HIS4, mek1Δ::LEU2::mek1Q241G::URA3, pch2Δ::NATMX4*
EAY3083	*MAT***a**, *ho::hisG, HIS4, mek1Δ::LEU2::mek1Q241G::URA3, spo11-HA::KANMX4*
EAY3084	*MATα, ho::hisG, HIS4, mek1Δ::LEU2::mek1Q241G::URA3, spo11-HA::KANMX4*
EAY3085	*MAT***a**, *ho::hisG, HIS4, mek1Δ::LEU2::mek1Q241G::URA3, pch2Δ::NATMX4, spo11-HA::KANMX4*
EAY3086	*MATα, ho::hisG, his4, mek1Δ::LEU2::mek1Q241G::URA3, pch2Δ::NATMX4, spo11-HA::KANMX4*
EAY3087	*MAT***a**, *ho::hisG, his4*
EAY3088	*MATα, ho::hisG, his4, ade2Δ*
EAY3089	*MAT***a**, *ho::hisG, HIS4, ura3, MEK1-GST-KANMX4*
EAY3090	*MATα, ho::hisG, his4, MEK1-GST-KANMX4*
EAY3091	*MAT***a**, *ho::hisG, his4, MEK1-GST-KANMX4, pch2Δ::NATMX4*
EAY3092	*MATα, ho::hisG, his4, MEK1-GST-KANMX4, pch2Δ::NATMX4*
EAY3093	*MAT***a**, *ho::hisG, his4, ura3, MEK1-GST-KANMX4, spo11-HA::KANMX4*
EAY3094	*MATα, ho::hisG, his4, ura3, MEK1-GST-KANMX4, spo11-HA::KANMX4*
EAY3095	*MAT***a**, *ho::hisG, his4, ura3, ade2Δ, leu2::hisG, MEK1-GST-KANMX4, pch2Δ::NATMX4, spo11-HA::KANMX4*
EAY3096	*MATα, ho::hisG, HIS4, ura3, MEK1-GST-KANMX4, pch2Δ::NATMX4, spo11-HA::KANMX4*

The diploid strain names are composites of the haploid strains used to create them.

Hochwagen *et al.* 2005; Wu and Burgess 2006; Mitra and Roeder 2007; Zanders and Alani 2009). On the basis of recent work showing a role for Pch2 in regulating crossing over in meiosis, we and others hypothesized that Pch2 acts directly in DSB repair (Hochwagen *et al.* 2005; Wu and Burgess 2006; Borner *et al.* 2008; Joshi *et al.* 2009; Zanders

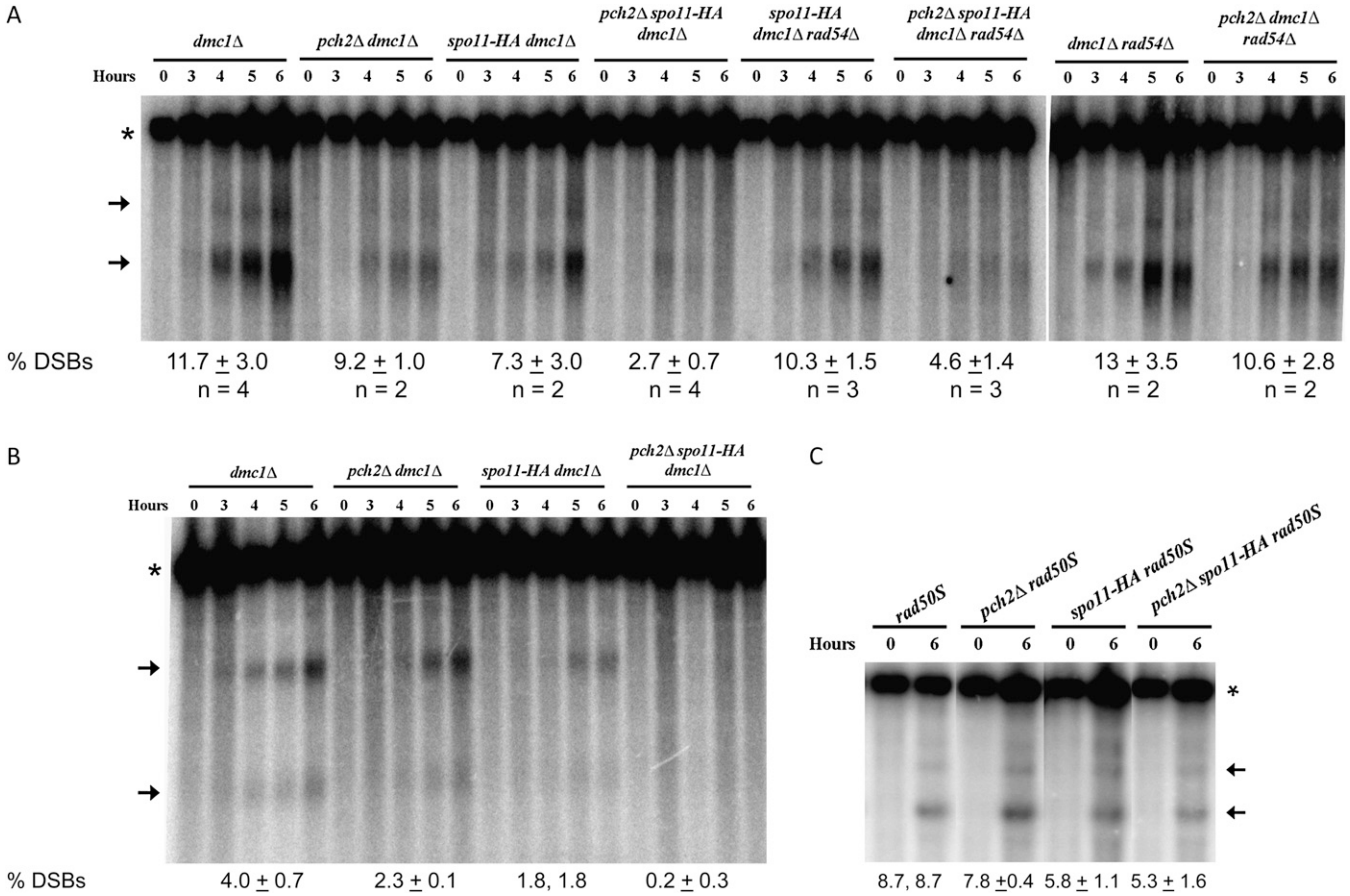

Figure 1 DSB levels observed at the *YCRO48W* and *HIS2* hotspots. (A) Southern blots were performed on genomic DNA obtained from 0-, 3-, 4-, 5-, and 6-hr postmeiotic induction of the indicated strains to measure DSBs at the *YCR048W* hotspot on chromosome III (Zanders and Alani 2009). DNA was digested with *Bgl*II and probed with a chromosome III fragment (SGD coordinates 215,422–216,703). Representative blots of independent replicates ($n = 2$ to 4) are shown. Asterisk denotes the 11-kb parental band, and the arrows designate the DSB bands quantified. The percentage of DSBs (percentage of total lane signal) at 6 hr ± standard deviation (SD) is shown for each strain. (B) Methods used in A were performed to measure DSBs at the *HIS2* hotspot on chromosome VI. The DNA was digested with *Bgl*II and probed as in Bullard *et al.* (1996). The asterisk denotes the 5-kb parental band and the arrows designate the DSB bands quantified. The percentage of DSBs (percentage of total lane signal) at 6 hr ± SD ($n = 2$) is shown for each strain. SD is not shown for *spo11-HA pch2*Δ because the same percentage of DSB value was obtained in two independent experiments. (C) Southern blots were performed on genomic DNA as shown in A at the *YCR048W* hotspot in *rad50S* strains. A representative blot ($n = 2$) is shown with the percentage of DSBs (percentage of total lane signal) at 6 hr (±SD) also shown. An SD is not shown for *rad50S* because the same percentage of DSB value was obtained in two independent experiments. The asterisk denotes the 11-kb parental band, and the arrows designate the DSB bands quantified. For A–C, similar results were obtained in independent time courses extended to $T = 7$ hr.

and Alani 2009). In such a model, *pch2*Δ relieves the *dmc1*Δ arrest by allowing Dmc1-independent DSB repair. Below are physical and genetic studies that are consistent with Pch2 inhibiting DSB repair in *dmc1*Δ cells.

We analyzed visible meiotic DSBs at the *YCR048W* (chromosome III) and *HIS2* (chromosome VI) hotspots in *pch2*Δ, *dmc1*Δ, *spo11-HA, rad50S*, and *rad54*Δ strain backgrounds. Six hours after meiotic induction, *dmc1*Δ mutants averaged 11.7 ± 3.0% (±SD; $n = 4$ independent cultures) DSBs at *YCRO48W*. *pch2*Δ *dmc1*Δ (9.2 ± 1.0%, $n = 2$) and *spo11-HA dmc1*Δ (7.3 ± 3.0%, $n = 2$) mutants displayed slightly fewer DSBs at this hotspot. Consistent with previous results, the *pch2*Δ *spo11-HA dmc1*Δ triple mutant showed lower DSB levels (2.7 ± 0.7%, $n = 4$; Figure 1A; Zanders and Alani 2009). A similar pattern of DSBs was observed at the *HIS2* DSB hotspot on chromosome VI (Figure 1B) (Bullard *et al.* 1996).

One explanation for the reduced level of breaks observed in *pch2*Δ *spo11-HA dmc1*Δ mutants is that fewer DSBs are formed in *pch2*Δ mutants. Previous genetic analyses, however, suggest that *pch2*Δ mutants do not form fewer DSBs; *pch2*Δ mutants have increased COs on large chromosomes and increased gene conversion frequencies on chromosomes of all sizes. The opposite effect would be expected from a mutant with reduced DSB frequencies (Zanders and Alani 2009). To formally test if *pch2*Δ *spo11-HA dmc1*Δ mutants affect DSB formation, we measured DSBs in the *rad50S* mutant background in which they persist (Alani *et al.* 1990). At the *YCR048w* hotspot, *rad50S* and *pch2*Δ *rad50S* mutants showed similar average DSB levels: 8.7% (same value in

Table 2 Spore formation efficiency and viability in *pch2*Δ mutants

Genotype	% sporulation	No. analyzed	% spore viability	Spores analyzed
Wild type	79.1	436	93.5	400
pch2Δ	80.9	429	95.3	400
spo11-HA	81.1	434	92.5	400
pch2Δ spo11-HA	74.9	453	56.8	400
dmc1Δ	0.0	406	NA	NA
pch2Δ dmc1Δ	4.6	431	2.9	148
spo11-HA dmc1Δ	0.4	239	NA	NA
pch2Δ spo11-HA dmc1Δ	39.0	439	1.3	160
spo11-HA/spo11yf-HA	79.6	421	ND	ND
pch2Δ/pch2Δ; spo11-HA/spo11yf-HA	67.7	440	ND	ND
spo11-HA/spo11yf-HA; dmc1Δ/dmc1Δ	4.6	415	ND	ND
pch2Δ/pch2Δ; spo11-HA/spo11yf-HA; dmc1Δ/dmc1Δ	42.8	523	ND	ND
rad54Δ	58.3	439	59.5	400
pch2Δ rad54Δ	46.0	443	47.0	400
spo11-HA rad54Δ	63.5	425	62.8	400
pch2Δ spo11-HA rad54Δ	30.7	440	38.0	400
dmc1Δ rad54Δ	0.2	422	NA	NA
pch2Δ dmc1Δ rad54Δ	0.0	444	NA	NA
spo11-HA dmc1Δ rad54Δ	0.0	409	NA	NA
pch2Δ spo11-HA dmc1Δ rad54Δ	0.0	403	NA	NA
spo13	63.3	441	47.3	400
pch2Δ spo13	49.2	417	44.8	400
spo11-HA spo13	51.8	454	44.8	400
pch2Δ spo11-HA spo13	56.9	457	44.3	400
dmc1Δ spo13	9.6	428	7.3	400
pch2Δ dmc1Δ spo13	43.4	422	15.5	400
spo11-HA dmc1Δ spo13	16.6	441	16.0	400
pch2Δ spo11-HA dmc1Δ spo13	57.9	480	25.5	396
pch2Δ spo11-HA dmc1Δ rad54Δ spo13	14.0	222	0.0	120

Sporulation efficiencies for the above strains were counted after 5 days on sporulation media at 30°. Tetrads (for *SPO13* strains) or dyads (from *spo13* strains) were dissected on YPD and scored for spore viability after 3 days. NA indicates that the percentage of spore viability is not applicable for strains that do not sporulate. ND indicates that spore viability was not assayed.

two independent experiments) and 7.8 ± 0.4%, respectively ($n = 2$; Figure 1C). The *spo11-HA rad50S* (5.8 ± 1.1%) and *pch2Δ spo11-HA rad50S* mutants (5.3 ± 1.6%) also showed similar levels of DSBs, although the levels were lower than *rad50S* alone, as expected because of the presence of *spo11-HA* ($n = 2$; Figure 1C). These results suggest that the decrease in DSBs observed in *pch2Δ spo11-HA dmc1Δ* was not due to a decrease in DSB formation.

Low levels of DSBs were observed in *pch2Δ spo11-HA dmc1Δ*. Interestingly, these strains showed a dramatic increase in meiotic completion—39% spore formation, compared to 0% in *dmc1Δ* strains, which showed high levels of DSBs (Bishop *et al.* 1999) (Table 2; $P < 0.005$; Figure 1). The *pch2Δ* and *spo11-HA* mutations contribute synergistically to the triple-mutant phenotype because only a small percentage of *pch2Δ dmc1Δ* (4.6%) and *spo11-HA dmc1Δ* (0.4%) cells formed spores. One explanation for the phenotype is that the recombination checkpoint is sensitive to the level of unrepaired breaks (see Discussion), such that fewer breaks elicit a less robust checkpoint arrest. Consistent with this interpretation, *dmc1Δ/dmc1Δ spo11-HA/spo11yf-HA* (30% of wild-type DSB levels) have increased meiotic progression [*dmc1Δ*, 0% spore formation; *spo11-HA/spo11yf-HA dmc1Δ/dmc1Δ*, 5% spore formation (Table 2; $P < 0.005$)].

Spores produced by *pch2Δ dmc1Δ* and *spo11-HA pch2Δ dmc1Δ* were mostly inviable (<3% spore viability for each), suggesting that interhomolog recombination was not restored in these mutants (Table 2). We tested whether other types of repair occurred in the *spo13* mutant background in which a mixed chromosome division occurs: some chromosomes undergo an equational division whereas others segregate reductionally (Klapholz and Esposito 1980; Hugerat and Simchen 1993). *spo13* mutants can produce viable meiotic progeny in the absence of meiotic DSBs or if DSB repair does not yield COs (*e.g.*, Malone and Esposito 1981). Because of this, spore viability analyses in the *spo13* mutant background can detect DSB repair that does not facilitate proper MI chromosome segregation (Bishop *et al.* 1999).

Similar to previous work in SK1 strains, *spo13 dmc1Δ* showed low levels of sporulation (10%) and spore viability

(7%) compared to *spo13* (63% sporulation, 47% viability; Table 2; $P < 0.005$ for both sporulation and spore viability) (Bishop *et al.* 1999). Introducing the *spo11-HA* allele to *dmc1Δ spo13* increased spore formation in the resulting triple mutant to 17% and spore viability to 16% (Table 2; $P < 0.005$ for both sporulation and spore viability). This result is expected because fewer DSBs are produced in *spo11-HA* strains (Martini *et al.* 2006; Johnson *et al.* 2007). Deleting *PCH2* in *dmc1Δ spo13* had a strong effect; sporulation in this triple mutant increased to 43% and spore viability increased to 16% (Table 2; $P < 0.005$ for both sporulation and spore viability). The *spo11-HA pch2Δ spo13 dmc1Δ* quadruple mutant showed even greater sporulation (58%) and spore viability (26%; Table 2; $P < 0.005$ for both sporulation and spore viability). These results are consistent with some Dmc1-independent repair occurring in *pch2Δ dmc1Δ* mutants.

pch2Δ mutants have an increased dependence on Rad54-mediated repair

Sporulation of *pch2Δ spo11-HA dmc1Δ* mutants and spore viability of the *pch2Δ spo11-HA dmc1Δ spo13* mutants were Rad54-dependent, suggesting that Rad54 is repairing breaks in these mutants (Table 2). During vegetative growth, DSBs are preferentially repaired by homologous recombination involving sister chromatids in steps that are mediated by the Rad51 recombinase and its partner Rad54 (Kadyk and Hartwell 1992; M. Shinohara *et al.* 1997; Arbel *et al.* 1999; Krogh and Symington 2004). Consistent with Rad54-dependent recombination in *pch2Δ* mutants, we observed a reduction in sporulation (46%) and spore viability (47%) in the *pch2Δ rad54Δ* double mutant compared to *pch2Δ* (81% sporulation and 95% spore viability) and *rad54Δ* single mutants (58% sporulation and 60% spore viability; Table 2; $P < 0.005$ for all comparisons). Interestingly, CO levels were not reduced in *pch2Δ rad54Δ* compared to *pch2Δ*, suggesting the Rad54-dependent recombination in *pch2Δ* mutants is intersister (Table 3).

An important prediction of the above genetic analyses is that the *rad54Δ* mutation should result in a restoration of observed DSBs in the *pch2Δ spo11-HA dmc1Δ* mutant. This prediction was not met; 4.6 ± 1.4% DSBs ($n = 3$) were observed at *YCRO48W* in *pch2Δ spo11-HA dmc1Δ rad54Δ*, compared to 2.7 ± 0.7% ($n = 4$) in *pch2Δ spo11-HA dmc1Δ* and 10.3 ± 1.5% ($n = 3$) in *spo11-HA dmc1Δ rad54Δ* 6 hr after meiotic induction (Figure 1). It is possible that both Dmc1- and Rad54-independent repair can occur in the absence of these factors in a *pch2Δ* background. Another possibility is that hyper-resected DSBs form in *pch2Δ spo11-HA dmc1Δ rad54Δ* that cannot be detected by Southern blot. More experimentation is needed to understand this phenotype.

pch2Δ spo11-HA phenotype is modulated by Mek1 activity

Previously, we showed (Zanders and Alani 2009) that *pch2Δ spo11-HA* strains have a spore viability defect and hypothesized that the decreased spore viability was due to defects in CO interference and partner choice. If a compromised interhomolog bias contributes to the *pch2Δ spo11-HA* phenotype, then further undermining interhomolog bias should enhance the phenotype. Alternatively, reinforcing interhomolog bias should suppress the *pch2Δ spo11-HA* phenotype. To test this hypothesis, we utilized two *MEK1* alleles: *mek1-as* (*mek1-Q241G* hypomorph) (Callender and Hollingsworth 2010) and *MEK1-GST* (hypermorph) (Wu *et al.* 2010). *mek1-as* strains complete meiosis efficiently in the absence of a 1-Na-PP1 inhibitor and display nearly wild-type spore viability; however, Mek1-as has reduced affinity for ATP *in vitro*, and in one *dmc1Δ* strain background, the *mek1-as*

Table 3 *pch2Δ* and *pch2Δ rad54Δ* display similar meiotic crossover levels

	Total spores	Recombinant	Parental	% recombinant
		Chromosome III		
HIS3-LEU2				
Wild type	2711	351	2360	12.9
pch2Δ	2691	389	2302	14.5
pch2Δ rad54Δ	458	62	396	13.5
LEU2-CEN3				
Wild type	2711	184	2527	6.8
pch2Δ	2691	241	2450	9.0
pch2Δ rad54Δ	458	41	417	9.0
CEN3-MAT				
Wild type	2711	402	2309	14.8
pch2Δ	2691	374	2317	13.9
pch2Δ rad54Δ	458	65	393	14.2
		Chromosome VII		
TRP5-CYH2				
Wild type	2711	908	1803	33.5
pch2Δ	2691	1149	1542	42.7
pch2Δ rad54Δ	458	199	259	43.4
CYH2-MET13				
Wild type	2711	260	2451	9.6
pch2Δ	2691	469	2222	17.4
pch2Δ rad54Δ	458	81	377	17.7
MET13-LYS5				
Wild type	2711	559	2152	20.6
pch2Δ	2691	747	1944	27.8
pch2Δ rad54Δ	458	139	319	30.3
		Chromosome VIII		
CEN8-THR1				
Wild type	2711	606	2105	22.4
pch2Δ	2691	649	2042	24.1
pch2Δ rad54Δ	458	116	342	25.3
THR1-CUP1				
Wild type	2711	668	2043	24.6
pch2Δ	2691	948	1743	35.2
pch2Δ rad54Δ	458	123	335	26.9

Wild-type (NH942/NH943), *pch2Δ* (EAY2209/EAY2210), and *pch2Δ rad54Δ* (EAY2681/EAY2685) strains were sporulated and analyzed for segregation of genetic markers in the NH942/NH943 strain background. Crossover frequencies in this strain were calculated from recombination frequencies in spores as described previously (Zanders and Alani 2009). Data for wild type and *pch2Δ* are from Zanders and Alani (2009). Spore viability was 91% for wild type (n =743 tetrads dissected), 97% for *pch2Δ* (n = 707 tetrads), and 45% for *pch2Δ rad54Δ* (n = 256 tetrads).

Table 4 Spore formation efficiency and viability in *mek1-as and MEK1-GST* mutants

Genotype	% sporulation	No. analyzed	% spore viability	Spores analyzed
Wild type	79.1	436	93.5	400
pch2Δ	80.9	429	95.3	400
spo11-HA	81.1	434	92.5	400
mek1-as	84.7	163	98.8	80
MEK1-GST	66.9	178	87.5	160
pch2Δ spo11-HA	74.9	453	56.8	400
mek1-as spo11-HA	87.8	164	92.3	400
mek1-as pch2Δ	88.5	191	92.0	400
MEK1-GST spo11-HA	69.8	162	85.4	546
MEK1-GST pch2Δ	67.5	155	86.5	408
pch2Δ spo11-HA mek1-as	85.8	183	40.8	400
pch2Δ spo11-HA MEK1-GST	63.5	143	89.0	552

Sporulation efficiencies for the above strains were counted after 5 days on sporulation media at 30°. Tetrads were dissected on YPD and scored for spore viability after 3 days.

mutation conferred phenotypes consistent with defects in interhomolog bias (Wan *et al.* 2004; Niu *et al.* 2009; Callender and Hollingsworth 2010). Wu *et al.* (2010) recently showed that *MEK1-GST* is a semidominant allele that shows increased interhomolog recombination events, primarily noncrossovers, and fewer intersister events, with no change in DSB levels.

As shown in Table 4, we constructed *mek1-as pch2Δ spo11-HA* and *MEK1-GST pch2Δ spo11-HA* strains and examined their spore formation efficiency and viability (*mek1-as* strains were analyzed in the absence of a 1-Na-PP1 inhibitor). We found that the *mek1-as* mutation reduced the spore viability of *pch2Δ spo11-HA* strains from 57 to 41% ($P < 0.005$). The *mek1-as* mutation did not significantly affect the spore viability of either single mutant alone (Table 4). The *MEK1-GST* allele increased spore viability in *pch2Δ spo11-HA* strains from 57 to 89% ($P < 0.005$); however, as described previously (Wu *et al.* 2010), there was a general defect in spore formation due to *MEK1-GST*. *MEK1-GST* did not increase the spore viability in either single mutant (Table 4). These data are consistent with our hypothesis that excess intersister repair contributes to spore inviablity of *pch2Δ spo11-HA*.

Evidence that Pch2 promotes interhomolog DSB repair

To more directly test if there is an increase in intersister repair in *pch2Δ*, we adapted an assay developed by Fasullo and Davis (1987) to measure sister-chromatid exchange in meiosis. This assay utilizes a *HIS3* reporter gene in which cells become His^+ if a sister-chromatid recombination event (either a CO or gene conversion) occurs between two *his3* truncations to produce full-length *HIS3*. The mean frequency of His^+ colonies was 1.6×10^{-6} ($n = 22$ independent cultures) in wild type and 5.3×10^{-6} in cells lacking Pch2 ($n = 24$). *pch2Δ* values were significantly higher than wild type ($P = 0.008$, Mann–Whitney *U*-test).

Discussion

We provide several independent lines of evidence consistent with a role for Pch2 in inhibiting Dmc1-independent intersister DSB repair in meiosis. First, *pch2Δ* contributes to a reduction of unrepaired DSBs visible on Southern blots in *spo11-HA dmc1Δ* mutants (Figure 1). This reduction in detectable DSBs appears to be due to DSB repair because the levels of DSBs formed, as measured in a *rad50S* background, are not affected by *pch2Δ* and the spore inviability seen in *pch2Δ dmc1Δ* and *pch2Δ spo11-HA dmc1Δ* mutants is suppressed by *spo13Δ* (Table 2). We hypothesize that the DSB repair occurring in *pch2Δ spo11-HA dmc1Δ* is intersister because it does not facilitate proper MI chromosome segregation. Our epistasis analysis of *pch2Δ rad54Δ* suggests that *pch2Δ* mutants are more dependent on Rad54-dependent repair, but that Rad54 does not appear to contribute to interhomolog CO repair in *pch2Δ*. These data further support the idea that *pch2Δ* mutants have increased intersister repair. In addition, we demonstrated that a *mek1* hypomorph enhanced the spore death phenotype of *pch2Δ spo11-HA* whereas a *MEK1* gain-of-function allele suppressed the phenotype. These experiments are consistent with excess intersister DSB repair contributing to spore inviability of *pch2Δ spo11-HA*. Finally, our genetic reporter assay demonstrated an increase in intersister DSB repair at one locus.

Our data and those of other groups are consistent with recombination checkpoint signaling being sensitive to unrepaired DSB levels, such that more DSBs trigger checkpoint arrest in a greater proportion of the cell population (Malkova *et al.* 1996; Bhalla and Dernburg 2005; MacQueen *et al.* 2005; Johnson *et al.* 2007; Callender and Hollingsworth 2010; Goldfarb and Lichten 2010). In wild-type cells, DSBs are quickly repaired and the Mek1-mediated checkpoint delay is transient. In *dmc1Δ*, DSBs are not repaired and Mek1 elicits checkpoint arrest. When DSBs are reduced in *dmc1Δ* strains containing *spo11* hypomorph alleles, the checkpoint response is less robust and fewer cells arrest. We hypothesize that the *spo11-HA* and *pch2Δ* mutations independently contribute to reducing the level of unrepaired DSBs available to trigger the recombination checkpoint in *dmc1Δ* mutants: *spo11-HA* forms fewer DSBs and *pch2Δ* acts by allowing Dmc1-independent repair. In this model, the combination of *spo11-HA* and *pch2Δ* in a *dmc1Δ* background synergistically contribute to DSB repair due to a positive feedback loop wherein fewer DSBs elicit less checkpoint activation, which allows even more DSB repair and meiotic progression. At present we do not have a good sense of the number of DSBs that would be needed to elicit checkpoint activation; however, work from Malkova *et al.* (1996) showed that a single unrepaired DSB does not arrest meiosis.

Pch2 acts in meiotic CO control to limit CO formation on large chromosomes and promote CO interference (Joshi *et al.* 2009; Zanders and Alani 2009). This work suggests a broader role for Pch2 in DSB repair that includes inhibiting

intersister DSB repair. Although the mechanism of Pch2 function in DSB repair is unknown, there are several avenues worthy of investigation. RTEL-1, the *Caenorhabditis elegans* homolog of the yeast Srs2 helicase has been shown to be defective in CO interference and CO homeostasis (Youds *et al.* 2010). Thus one possibility is that Pch2 facilitates access of a helicase to remove inappropriate strand invasion events. Borner *et al.* (2008) first posited another attractive (and not mutually exclusive) hypothesis that Pch2 somehow promotes Mec1 regulatory action. Indeed, at least one Mek1 effector (a Mec1 target) that promotes interhomolog bias is still unknown (Niu *et al.* 2009; Hollingsworth 2010). This effector could be Pch2 acting to augment or promote Mek1 activity. Under this model, Mek1 signaling is attenuated in *pch2*Δ mutants, allowing excess intersister repair. Such an idea is consistent with work from Wu *et al.* (2010), who showed that an activated *MEK1* allele (*MEK1-GST*) promoted an increase in interhomolog events that were primarily repaired as NCOs and fewer intersister events, with no change in DSB levels (Wu *et al.* 2010). This idea is also consistent with previous data showing that *pch2*Δ mutants display increased CO events at the expense of NCOs (Zanders and Alani 2009). Experiments to test these hypotheses are underway.

Acknowledgments

We are grateful to Valentin Boerner, Andreas Hochwagen, Michael Lichten, and Scott Keeney for providing unpublished data and to Chip Aquadro, Joshua Filter, Heather Flores, Tamara Goldfarb, Nancy Hollingsworth, and Michael Lichten for critical comments and technical advice. We thank Mike Fasullo for providing the *HIS3* sister-chromatid exchange plasmid and Nancy Hollingsworth and Sean Burgess for providing the *mek1-as* and *MEK1-GST* alleles, respectively. Finally, we are grateful to Nancy Hollingsworth for helpful discussions. This work was supported by National Institutes of Health (NIH) grant GM53085 supplemented with an American Recovery and Reinvestment Act award (to E.A.). S.Z. and M.S.B. were supported by NIH training grants awarded to Cornell University.

Literature Cited

Alani, E., R. Padmore, and N. Kleckner, 1990 Analysis of wild-type and *rad50* mutants of yeast suggests an intimate relationship between meiotic chromosome synapsis and recombination. Cell 61: 419–436.

Arbel, A., D. Zenvirth, and G. Simchen, 1999 Sister chromatid-based DNA repair is mediated by *RAD54*, not by *DMC1* or *TID1*. EMBO J. 18: 2648–2658.

Argueso, J. L., J. Wanat, Z. Gemici, and E. Alani, 2004 Competing crossover pathways act during meiosis in *Saccharomyces cerevisiae*. Genetics 168: 1805–1816.

Berchowitz, L. E., and G. P. Copenhaver, 2010 Genetic interference: don't stand so close to me. Curr. Genomics 11: 91–102.

Bhalla, N., and A. F. Dernburg, 2005 A conserved checkpoint monitors meiotic chromosome synapsis in *Caenorhabditis elegans*. Science 310: 1683–1686.

Bishop, D. K., and D. Zickler, 2004 Early decision: meiotic crossover interference prior to stable strand exchange and synapsis. Cell 117: 9–15.

Bishop, D. K., D. Park, L. Xu, and N. Kleckner, 1992 *DMC1*: a meiosis-specific yeast homolog of *E. coli recA* required for recombination, synaptonemal complex formation, and cell cycle progression. Cell 69: 439–456.

Bishop, D. K., Y. Nikolski, J. Oshiro, J. Chon, M. Shinohara *et al.*, 1999 High copy number suppression of the meiotic arrest caused by a *dmc1* mutation: *REC114* imposes an early recombination block and *RAD54* promotes a *DMC1*-independent DSB repair pathway. Genes Cells 4: 425–444.

Blitzblau, H. G., G. W. Bell, J. Rodriguez, S. P. Bell, and A. Hochwagen, 2007 Mapping of meiotic single-stranded DNA reveals double-stranded-break hotspots near centromeres and telomeres. Curr. Biol. 17: 2003–2012.

Borner, G. V., N. Kleckner, and N. Hunter, 2004 Crossover/noncrossover differentiation, synaptonemal complex formation, and regulatory surveillance at the leptotene/zygotene transition of meiosis. Cell 117: 29–45.

Borner, G. V., A. Barot, and N. Kleckner, 2008 Yeast Pch2 promotes domainal axis organization, timely recombination progression, and arrest of defective recombinosomes during meiosis. Proc. Natl. Acad. Sci. USA 105: 3327–3332.

Buhler, C., V. Borde, and M. Lichten, 2007 Mapping meiotic single-strand DNA reveals a new landscape of DNA double-strand breaks in *Saccharomyces cerevisiae*. PLoS Biol. 5: e324.

Bullard, S. A., S. Kim, A. M. Galbraith, and R. E. Malone, 1996 Double strand breaks at the *HIS2* recombination hot spot in *Saccharomyces cerevisiae*. Proc. Natl. Acad. Sci. USA 93: 13054–13059.

Busygina, V., M. G. Sehorn, I. Y. Shi, H. Tsubouchi, G. S. Roeder *et al.*, 2008 Hed1 regulates Rad51-mediated recombination via a novel mechanism. Genes Dev. 22: 786–795.

Callender, T., and N. M. Hollingsworth, 2010 Mek1 suppression of meiotic double-strand break repair is specific to sister chromatids, chromosome autonomous and independent of Rec8 cohesin complexes. Genetics 185: 771–782.

Carballo, J. A., A. L. Johnson, S. G. Sedgwick, and R. S. Cha, 2008 Phosphorylation of the axial element protein Hop1 by Mec1/Tel1 ensures meiotic interhomolog recombination. Cell 132: 758–770.

Chen, S. Y., T. Tsubouchi, B. Rockmill, J. S. Sandler, D. R. Richards *et al.*, 2008 Global analysis of the meiotic crossover landscape. Dev. Cell 15: 401–415.

De los Santos, T., N. Hunter, D. Lee, B. Larkin, J. Loidl *et al.*, 2003 The Mus81/Mms4 endonuclease acts independently of double-Holliday junction resolution to promote a distinct subset of crossovers during meiosis in budding yeast. Genetics 164: 81–94.

De Massy, B., F. Baudat, and A. Nicolas, 1994 Initiation of recombination in *Saccharomyces cerevisiae* haploid meiosis. Proc. Natl. Acad. Sci. USA 91: 11929–11933.

Dresser, M. E., D. J. Ewing, M. N. Conrad, A. M. Dominguez, R. Barstead *et al.*, 1997 *DMC1* functions in a *Saccharomyces cerevisiae* meiotic pathway that is largely independent of the *RAD51* pathway. Genetics 147: 533–544.

Fasullo, M. T., and R. W. Davis, 1987 Recombinational substrates designed to study recombination between unique and repetitive sequences in vivo. Proc. Natl. Acad. Sci. USA 84: 6215–6219.

Gietz, R. D., R. H. Schiestl, A. R. Willems, and R. A. Woods, 1995 Studies on the transformation of intact yeast cells by the LiAc/SS-DNA/PEG procedure. Yeast 11: 355–360.

Goldfarb, T., and M. Lichten, 2010 The sister chromatid is frequently and efficiently used for DNA double-strand break repair during budding yeast meiosis. PLoS Biol. 8: e1000520.

Goldstein, A. L., and J. H. McCusker, 1999 Three new dominant drug resistance cassettes for gene disruption in *Saccharomyces cerevisiae*. Yeast 15: 1541–1553.

Goyon, C., and M. Lichten, 1993 Timing of molecular events in meiosis in *Saccharomyces cerevisiae*: stable heteroduplex DNA is formed late in meiotic prophase. Mol. Cell. Biol. 13: 373–382.

Hassold, T., H. Hall, and P. Hunt, 2007 The origin of human aneuploidy: where we have been, where we are going. Hum. Mol. Genet. 16: R203–R208.

Hochwagen, A., W. H. Tham, G. A. Brar, and A. Amon, 2005 The FK506 binding protein Fpr3 counteracts protein phosphatase 1 to maintain meiotic recombination checkpoint activity. Cell 122: 861–873.

Hollingsworth, N. M., 2010 Phosphorylation and the creation of interhomolog bias during meiosis in yeast. Cell Cycle 9: 436–437.

Hollingsworth, N. M., and B. Byers, 1989 *HOP1*: a yeast meiotic pairing gene. Genetics 121: 445–462.

Hollingsworth, N. M., L. Goetsch, and B. Byers, 1990 The *HOP1* gene encodes a meiosis-specific component of yeast chromosomes. Cell 61: 73–84.

Hugerat, Y., and G. Simchen, 1993 Mixed segregation and recombination of chromosomes and YACs during single-division meiosis in *spo13* strains of *Saccharomyces cerevisiae*. Genetics 135: 297–308.

Jackson, J. A., and G. R. Fink, 1985 Meiotic recombination between duplicated genetic elements in *Saccharomyces cerevisiae*. Genetics 109: 303–332.

Johnson, R., V. Borde, M. J. Neale, A. Bishop-Bailey, M. North *et al.*, 2007 Excess single-stranded DNA inhibits meiotic double-strand break repair. PLoS Genet. 3: e223.

Jones, G. H., and F. C. Franklin, 2006 Meiotic crossing-over: obligation and interference. Cell 126: 246–248.

Joshi, N., A. Barot, C. Jamison, and G. V. Borner, 2009 Pch2 links chromosome axis remodeling at future crossover sites and crossover distribution during yeast meiosis. PLoS Genet. 5: e1000557.

Kadyk, L. C., and L. H. Hartwell, 1992 Sister chromatids are preferred over homologs as substrates for recombinational repair in *Saccharomyces cerevisiae*. Genetics 132: 387–402.

Klapholz, S., and R. E. Esposito, 1980 Isolation of *SPO12-1* and *SPO13-1* from a natural variant of yeast that undergoes a single meiotic division. Genetics 96: 567–588.

Klein, H. L., 1997 *RDH54*, a *RAD54* homologue in *Saccharomyces cerevisiae*, is required for mitotic diploid-specific recombination and repair and for meiosis. Genetics 147: 1533–1543.

Krogh, B. O., and L. S. Symington, 2004 Recombination proteins in yeast. Annu. Rev. Genet. 38: 233–271.

Li, X. C., and J. Schimenti, 2007 Mouse pachytene checkpoint 2 (*trip13*) is required for completing meiotic recombination but not synapsis. PLoS Genet. 3: e130.

Lydall, D., Y. Nikolsky, D. K. Bishop, and T. A. Weinert, 1996 A meiotic recombination checkpoint controlled by mitotic checkpoint genes. Nature 383: 840–843.

MacQueen, A. J., C. M. Phillips, A. Bhalla, P. Weiser, A. M. Villeneuve *et al.*, 2005 Chromosome sites play dual roles to establish homologous synapsis during meiosis in *C. elegans*. Cell 123: 1037–1050.

Malkova, A., L. Ross, D. Dawson, M. F. Hoekstra, and J. E. Haber, 1996 Meiotic recombination initiated by a double-strand break in *rad50* delta yeast cells otherwise unable to initiate meiotic recombination. Genetics 143: 741–754.

Malone, R. E., and R. E. Esposito, 1981 Recombinationless meiosis in *Saccharomyces cerevisiae*. Mol. Cell. Biol. 1: 891–901.

Mancera, E., R. Bourgon, R. Brozzi, W. Huber, and L. M. Steinmetz, 2008 High-resolution mapping of meiotic crossovers and non-crossovers in yeast. Nature 454: 479–485.

Martini, E., R. L. Diaz, N. Hunter and S. Keeney, 2006 Crossover homeostasis in yeast meiosis. Cell 126: 285–295.

Mitra, N., and G. S. Roeder, 2007 A novel nonnull *ZIP1* allele triggers meiotic arrest with synapsed chromosomes in *Saccharomyces cerevisiae*. Genetics 176: 773–787.

Niu, H., L. Wan, B. Baumgartner, D. Schaefer, J. Loidl *et al.*, 2005 Partner choice during meiosis is regulated by Hop1-promoted dimerization of Mek1. Mol. Biol. Cell 16: 5804–5818.

Niu, H., X. Li, E. Job, C. Park, D. Moazed *et al.*, 2007 Mek1 kinase is regulated to suppress double-strand break repair between sister chromatids during budding yeast meiosis. Mol. Cell. Biol. 27: 5456–5467.

Niu, H., L. Wan, V. Busygina, Y. Kwon, J. A. Allen *et al.*, 2009 Regulation of meiotic recombination via Mek1-mediated Rad54 phosphorylation. Mol. Cell 36: 393–404.

Rockmill, B., and G. S. Roeder, 1990 Meiosis in asynaptic yeast. Genetics 126: 563–574.

Roeder, G. S., 1997 Meiotic chromosomes: it takes two to tango. Genes Dev. 11: 2600–2621.

Roig, I., J. A. Dowdle, A. Toth, D. G. De Rooj, M. Jasin *et al.*, 2010 Mouse TRIP13/PCH2 is required for recombination and normal higher order chromosome structure during meiosis. PLoS Genet. 6: e1001062.

San-Segundo, P. A., and G. S. Roeder, 1999 Pch2 links chromatin silencing to meiotic checkpoint control. Cell 97: 313–324.

Schwacha, A., and N. Kleckner, 1994 Identification of joint molecules that form frequently between homologs but rarely between sister chromatids during yeast meiosis. Cell 76: 51–63.

Schwacha, A., and N. Kleckner, 1997 Interhomolog bias during meiotic recombination: meiotic functions promote a highly differentiated interhomolog-only pathway. Cell 90: 1123–1135.

Shinohara, A., S. Gasior, T. Ogawa, N. Kleckner and D. K. Bishop, 1997 *Saccharomyces cerevisiae* recA homologs RAD51 and DMC1 have both distinct and overlapping roles in meiotic recombination. Genes Cells 2: 615–629.

Shinohara, M., E. Shita-Yamaguchi, J. M. Buerstedde, H. Shinagawa, H. Ogawa *et al.*, 1997 Characterization of the roles of the *Saccharomyces cerevisiae RAD54* gene and a homologue of *RAD54*, *RDH54/TID1*, in mitosis and meiosis. Genetics 147: 1545–1556.

Sym, M., and G. S. Roeder, 1995 Zip1-induced changes in synaptonemal complex structure and polycomplex assembly. J. Cell Biol. 128: 455–466.

Terentyev, Y., R. Johnson, M. J. Neale, M. Khisroon, A. Bishop-Bailey *et al.*, 2010 Evidence that MEK1 positively promotes interhomologue double-strand break repair. Nucleic Acids Res. 38: 4349–4360.

Thompson, D. A., and F. W. Stahl, 1999 Genetic control of recombination partner preference in yeast meiosis: isolation and characterization of mutants elevated for meiotic unequal sister-chromatid recombination. Genetics 153: 621–641.

Tsubouchi, H., and G. S. Roeder, 2003 The importance of genetic recombination for fidelity of chromosome pairing in meiosis. Dev. Cell 5: 915–925.

Tsubouchi, H., and G. S. Roeder, 2006 Budding yeast Hed1 down-regulates the mitotic recombination machinery when meiotic recombination is impaired. Genes Dev. 20: 1766–1775.

Wach, A., A. Brachat, R. Pohlmann and P. Philippsen, 1994 New heterologous modules for classical or PCR-based gene disruptions in *Saccharomyces cerevisiae*. Yeast 10: 1793–1808.

Wan, L., T. De los Santos, C. Zhang, K. Shokat, and N. M. Hollingsworth, 2004 Mek1 kinase activity functions downstream of *RED1* in the regulation of meiotic double strand break repair in budding yeast. Mol. Biol. Cell. 15: 11–23.

Webber, H. A., L. Howard, and S. E. Bickel, 2004 The cohesion protein ORD is required for homologue bias during meiotic recombination. J. Cell Biol. 164: 819–829.
Wojtasz, L., K. Daniel, I. Roig, E. Bolcun-Filas, H. Xu *et al.*, 2009 Mouse HORMAD1 and HORMAD2, two conserved meiotic chromosomal proteins, are depleted from synapsed chromosome axes with the help of TRIP13 AAA-ATPase. PLoS Genet. 5: e1000702.
Wu, H. Y., and S. M. Burgess, 2006 Two distinct surveillance mechanisms monitor meiotic chromosome metabolism in budding yeast. Curr. Biol. 16: 2473–2479.
Wu, H. Y., H. C. Ho, and S. M. Burgess, 2010 Mek1 kinase governs outcomes of meiotic recombination and the checkpoint response. Curr. Biol. 20: 1707–1716.
Xu, L., B. M. Weiner, and N. Kleckner, 1997 Meiotic cells monitor the status of the interhomolog recombination complex. Genes Dev. 11: 106–118.
Youds, J. L., D. G. Mets, M. J. Mcilwraith, J. S. Martin, J. D. Ward *et al.*, 2010 RTEL-1 enforces meiotic crossover interference and homeostasis. Science 327: 1254–1258.
Zanders, S., and E. Alani, 2009 The *pch2Delta* mutation in baker's yeast alters meiotic crossover levels and confers a defect in crossover interference. PLoS Genet. 5: e1000571.
Zierhut, C., M. Berlinger, C. Rupp, A. Shinohara, and F. Klein, 2004 Mnd1 is required for meiotic interhomolog repair. Curr. Biol. 14: 752–762.

Communicating editor: J. Engebrecht